

Supplementary Information

Osteocalcin Facilitates Calcium Phosphate Ion Complex Growth as Revealed by Free Energy Calculation

Weilong Zhao¹, Ziqiu Wang¹, Zhijun Xu², and Nita Sahai^{1,3*}

¹Department of Polymer Science, University of Akron, 170 University Ave, Akron, Ohio 44325-3909, United States.

²College of Chemical Engineering, State Key Laboratory of Materials-Oriented Chemical Engineering, Nanjing Tech University, Nanjing 210009, China.

³Department of Geology and Integrated Bioscience Program, University of Akron, Akron, Ohio 44325-3909, United States

Supplementary Experimental Procedure

DLS. All chemicals were purchased from Sigma-Aldrich™ at ACS reagent grade and ultrapure water ($\rho = 18.2 \text{ M}\Omega \cdot \text{cm}$) was used as the solvent. Separate calcium and phosphate solutions of 0.4 mM concentration each were prepared by dissolving calcium chloride (CaCl_2) and ammonium phosphate dibasic ($(\text{NH}_4)_2\text{HPO}_4$) separately in 10 mM HEPES buffer. Subsequently, OCN (fragment 1-49, human) was added to the calcium solution to reach a concentration of $20 \mu\text{g} \cdot \text{ml}^{-1}$. The pH of the phosphate solution and OCN-containing calcium solution was adjusted to 7.4 by sodium hydroxide. The solutions were then placed on a Stuart SB3 rotator at a speed of 50 rpm for 4 hours. After this incubation, the solutions were filtered through $0.2 \mu\text{m}$ membrane filters in order to minimize potential interference by adventitious dust particles in the following light scattering measurements. For the inorganic reference system, 0.4 mM calcium solution and phosphate solution were each adjusted to pH = 7.4 and filtered. Then,

the solutions were mixed together at a volume ratio of 1:1 in 1 ml BRAND UV-cuvette right before the DLS measurements to reach the following working concentrations: Ca^{2+} : 0.2 mM; HPO_4^{2-} : 0.2 mM; OCN: $10 \mu\text{g}\cdot\text{ml}^{-1}$. The DLS measurements were conducted on a ZetaSizer Nanoseries NS (Malvern Instrument, London, UK) using a backscattering angle of 173° at 20°C . Each data point was obtained based on 3 runs of 20 seconds duration. For both OCN-containing solution and control solution, 120 data points were collected over 4 hours, with 60 seconds delay between the adjacent points. Data fitting was performed by using both multimodal distribution and CONTIN models, both of which led to similar size distribution curves as a function of particle number probability.

Figure S1. 3-D structure of OCN used for modeling (PDB ID: 1q8h). Crystal structure of only residues 13 to 49 were available experimentally based on XRD data. The protein backbone and van der Waals surface are colored based on the hydrophobicity/charge of residues: white: non-polar; green: polar and neutral; red: negatively charged; blue: positively charged. Gla residues (γ E) are shown in ball-and-stick model. The sequence of human OCN is also shown, with the Gla residues colored by red, and phosphate-binding, charged side chain residues at the C-terminal colored by blue.

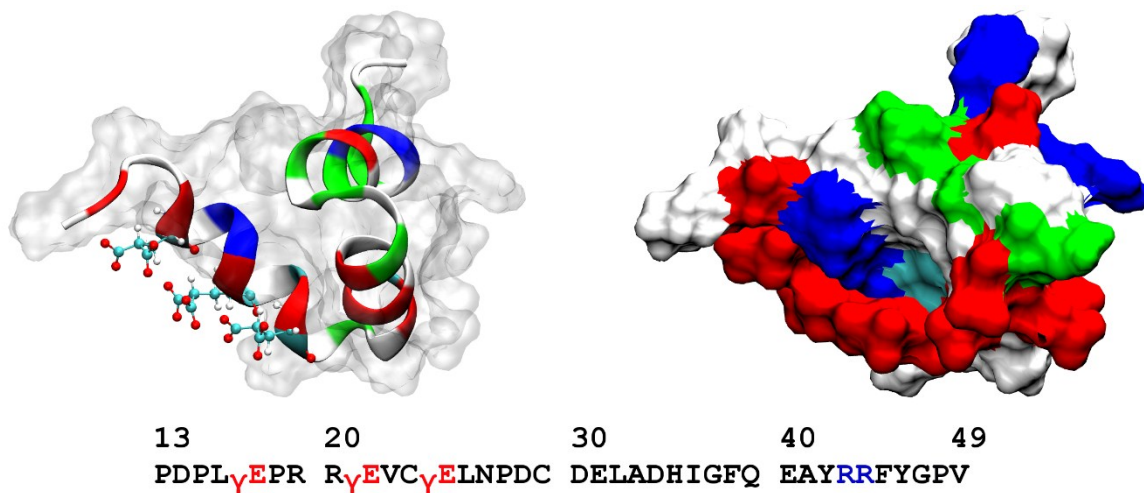


Figure S2. (a) Perspective views of simulation systems of Ion-Ref and Ion-OCN, visualized by VMD 1.9.1. Water molecules, Na^+ , and Cl^- ions are omitted for clarity. MetaD results of the Ion-Ref system are shown in the left panel. The complexes from the Ion-OCN system obtained by MetaD (middle panel) are larger than those by conventional MD (right panel). The boundaries of the simulation box are drawn in black lines. OCN backbone is shown in yellow ribbon. Calcium, phosphorus, and oxygen atoms are shown in cyan, tan, and red spheres, respectively. Simulation box is viewed from perspective angle and the boundaries are shown in black. (b) The MCS (left panel) and the average cluster size (right panel) as counted by the number of Ca^{2+} and HPO_4^{2-} ions within the complexes, are shown for the Ion-OCN system simulated by MetaD and conventional MD, and the Ion-Ref system simulated under MetaD. The Ion-Ref system simulated by conventional MD method has very similar results compared to MetaD and thus is not shown here. Note that for MetaD systems, the simulation timescale does not map to the actual physical timescale.

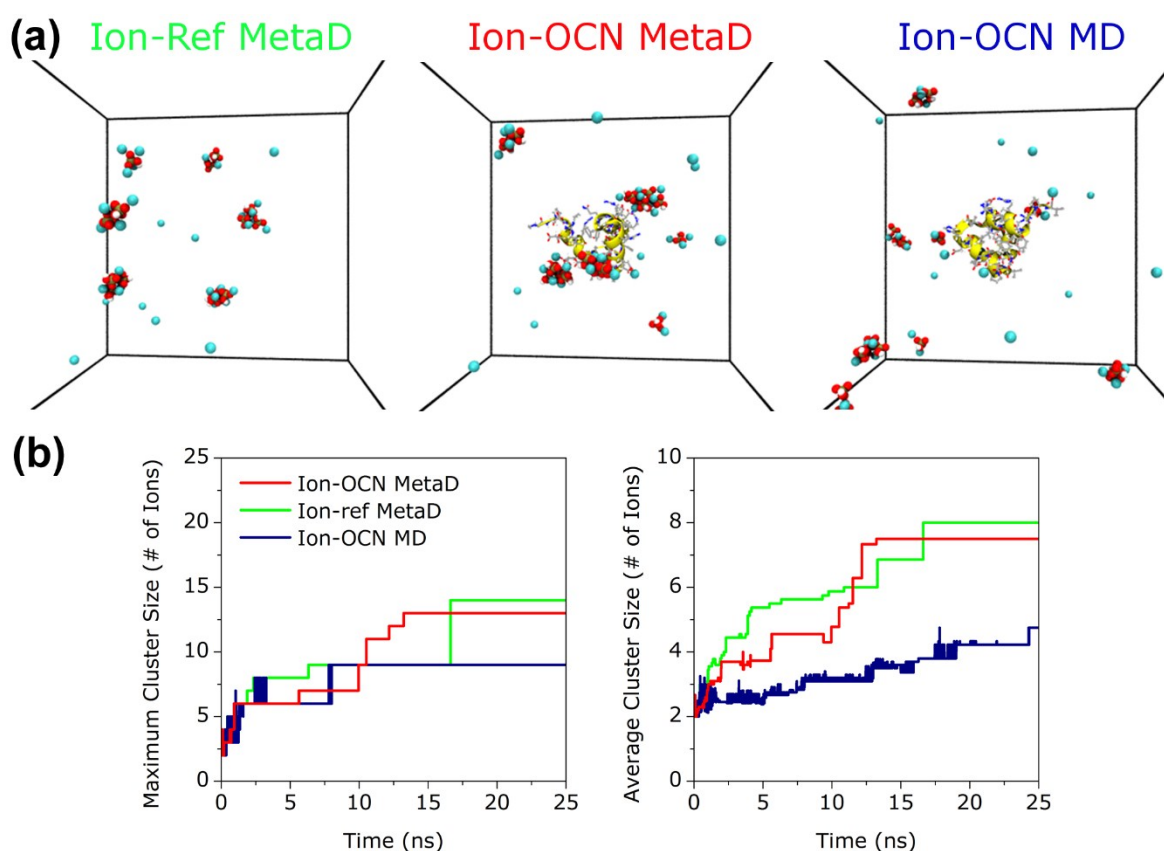


Figure S3. DLS results of CaP growth dynamics from IACs to large cluster assemblies and ACP particles. a) Size distribution of IACs from continuous DLS measurements over a 4-hour period. Each point was taken as the number mean size reported by the instrument. (b) Size distribution at different time points. Curves were fitted as a function of particle number probability based on CONTIN model.

